Rheol Acta
DOI 10.1007/s00397-011-0595-5

ORIGINAL CONTRIBUTION

Extensional-flow-induced crystallization of isotactic polypropylene

Erica E. Bischoff White · H. Henning Winter · Jonathan P. Rothstein

Received: 13 May 2011 / Revised: 16 August 2011 / Accepted: 5 September 2011

Abstract A filament stretching extensional rheometer with a custom-built oven was used to investigate the effect of uniaxial flow on the crystallization of polypropylene. Prior to stretching, samples were heated to a temperature well above the melt temperature to erase their thermal and mechanical histories and the Janeschitz-Kriegl protocol was applied. The samples were stretched at extension rates in the range of $0.01\,s^{-1} \leq \dot{\varepsilon} \leq 0.75\,s^{-1}$ to a final strain of $\varepsilon = 3.0$. After stretching, the samples were allowed to crystallize isothermally. Differential scanning calorimetry was applied to the crystallized samples to measure the degree of crystallinity. The results showed that a minimum extension rate is required for an increase in percent crystallization to occur and that there is an extension rate for which percent crystallization is maximized. No increase in crystallization was observed for extension rates below a critical extension rate corresponding to a Weissenberg number of approximately $Wi = 1$. Below this Weissenberg number, the flow is not strong enough to align the contour path of the polymer chains within the melt and as a result there is no change in the final percent crystallization from the quiescent state. Beyond this critical extension rate, the percent crystallization was observed to increase to a maximum, which was 18% greater than the quiescent case, before decaying again at higher extension rates. The increase in crystallinity is likely due to flow-induced orientation and alignment of contour path of the polymer chains in the flow direction. Polarized light microscopy verified an increase in number of spherulites and a decrease in spherulite size with increasing extension rate. In addition, small angle X-ray scattering showed a 7% decrease in inter-lamellar spacing at the transition to flow-induced crystallization. Although an increase in strain resulted in a slight increase in percent crystallization, no significant trends were observed. Crystallization kinetics were examined as a function of extension rate by observing the time required for molten samples to crystallize under uniaxial flow. The crystallization time was defined as the time at which a sudden increase in the transient force measurement was observed. The crystallization time was found to decrease as one over the extension rate, even for extension rates where no increase in percent crystallization was observed. As a result, the onset of extensional-flow-induced crystallization was found to occur at a constant value of strain equal to $\varepsilon_c = 5.8$.

Keywords Extensional flow · Polymer melt · Crystallization · Flow-induced orientation · Uniaxial extension

E. E. Bischoff White · J. P. Rothstein (✉)
Department of Mechanical and Industrial Engineering, University of Massachusetts, Amherst, MA 01003, USA
e-mail: rothstein@ecs.umass.edu

H. Henning Winter
Department of Chemical Engineering, University of Massachusetts, Amherst, MA 01003, USA

Introduction

Manufacturing of plastics is carried out through the application of various processing techniques including extrusion, blow molding, injection molding, casting,

Published online: 28 October 2011

fiber spinning, and rolling (Keller and Kolnaar 1997). All of these techniques rely on the application of heat and deformation of the material. The type and specifications of the process used to mold polymers has a significant impact on the properties of the final product. Many of these processes, such as blow molding and fiber spinning, primarily impose extensional flows on the polymer melt. Thus, understanding the rheological properties of and response of polymer melts in extensional flows is critical to a number of applications and industries.

The application of a sufficiently strong flow field to a polymer melt during processing will result in the alignment and in some cases the deformation of polymer chains. Flow is known to promote crystallization both by increasing the number of nucleation points for crystals to originate and by speeding up crystallization kinetics (Keller and Kolnaar 1997). For quickly crystallizing polymers, such as isotactic polypropylene, an increase in supercooling alone under quiescent conditions can result in a significant increase in the number of nucleation points (Janeschitz-Kriegl et al. 1995). The introduction of flow while in the supercooled state can have an even greater impact (Janeschitz-Kriegl 2003), reducing the time required to fully crystallize by several orders of magnitude (Haas and Maxwell 1969). This is because the flow-induced stretching and aligning of polymer chains reduces the entropy of the system as well as the change in free energy required for crystallization to take place (Mackley and Keller 1975). This results in an increase in the melting temperature of the polymer and an effective increase in the degree of supercooling. The extension of polymer chains also reduces the kinetic barrier which must be overcome for crystallization to occur because the deformed state of the polymer chain in the melt is closer to the state of the final crystal than a random coil (Keller and Kolnaar 1997).

Furthermore, when polymer chains are aligned and stretched in the flow direction, the polymer can form a shish-kebab crystal structure. In shish-kebabs, lamellar crystals grow outward from an aligned cylindrical core. In order for shish-kebabs to nucleate, sufficient chain extension and orientation is required and is typically characterized by a critical value of the specific work of the flow (Mackley 1975; Mykhaylyk et al. 2010; Van Puyvelde et al. 2008). Therefore, an elongational component must exist in the flow for a shish-kebab structure to evolve, whether it be in a purely extensional flow or a shear flow with a tangential velocity gradient that results in local chain extension. However, because shear flows result in a rotation of the polymer chains away from the direction of extension they are less effective at producing chain deformation than extensional flows (McKinley and Sridhar 2002a). As a result, the strain requirement for flow-induced crystallization is less in extension than it is in shear (Sentmanat et al. 2010). Even though extensional flows are able to generate greater molecular alignment than shear flows (Hadinata et al. 2007) and therefore more effectively enhance the resulting crystallization kinetics and morphological changes, very few studies have systematically investigated the effect of pure extensional flows on crystallization (Chellamuthu et al. 2011; Hadinata et al. 2007; Sentmanat et al. 2010).

Extensional flow can have a varying effect on the microstructure of a polymer, which is highly dependent on the strength of the flow. The Weissenberg number is used to characterize the strength of the flow. In order to calculate the Weissenberg number, the characteristic relaxation time of the fluid must first be determined. There are many relaxation times for entangled polymer systems; the ones of most interest for this study are the reptation or disengagement time, λ_d, and the Rouse time, λ_R. The disengagement time is a measure of the time it takes for the polymer chains to reptate past each other to relieve stress imposed by a flow. This relaxation time is used to calculate the Weissenberg number, $Wi = \lambda_d \dot{\varepsilon}$. The Rouse time, which is much shorter than the disengagement time, is the relaxation time for a polymer chain within its tube of entanglements. The Rouse time is a function of the average number of entanglements per chain of polymer, $Z = M_w/M_e$, and is given by $\lambda_R = \lambda_d/3Z$ (Doi and Edwards 1986). At low Weissenberg numbers, the flow is not strong enough to have any lasting effect and the polymer chains have time to relax. At $Wi \geq 1/2$, the flow becomes strong enough to align the contour path of the polymer chains. However, it is not until $Wi > \lambda_d/\lambda_R = 3Z$ that the polymer chains within their tubes of entanglements are extended and stretched. It has been shown in shear flow that for monodisperse polymers, the formation of shish-kebab morphologies are only possible for flows where $\dot{\gamma} > 1/\lambda_R$ (Mykhaylyk et al. 2011; van Meerveld et al. 2004). However, for polydisperse systems, shish-kebab morphologies can be generated if the specific work imposed by the flow is large enough to deform the higher molecular weight fractions of the melt (Mykhaylyk et al. 2010). This was recently observed in extensional flows by Chellamuthu et al. (2011) for a polydisperse poly-1-butene sample that developed a shish-kebab morphology even for extension rates less than one over the Rouse time, $\dot{\varepsilon} < 1/\lambda_R$.

Extensional-flow-induced crystallization was studied and compared to shear-flow-induced crystallization of a high molecular weight isotactic poly-1-butene by

Hadinata et al. (2007). They used an extensional viscosity fixture on a rotational rheometer (SER extensional rheometer) to apply an extensional flow to the melts. By marking the onset of crystallization to be the time at which a sudden increase in extensional viscosity was observed, they were able to deduce that flow-induced crystallization occurred in extension at 100th of the time it takes to occur under shear. They were also able to show that, after a critical extension rate, the onset of crystallization time decreased roughly with the inverse of the extension rate. They attributed this result to the extensional flows ability to orient polymer chains. At low extension rates, the flow was too slow to compete with the relaxation of the polymer and no change in crystallization time was observed. Their results demonstrate that extensional flow is a stronger agent for nucleating crystals than shear flow. In addition, they found that the onset of crystallization time, for extension rates of $\dot{\varepsilon} \geq 0.01\ s^{-1}$, did not vary with temperature. These results indicate that, kinetically, the crystallization kinetics were dominated by the applied flow field and not the underlying thermal motion of the polymer chains. Unfortunately, in their experiments they were unable to measure either the final percent crystallization or the final crystal structure due to sagging of the samples within their extensional rheometer (Hadinata et al. 2007). In this manuscript, the effect of extensional flow on the dynamics of crystallization will be studied for isotactic polypropylene by measuring the time for onset of crystallization using a filament stretching rheometer.

In a more recent experiment, Sentmanat et al. (2010) used a similar SER extensional rheometer to apply uniaxial extensional flow to an ethylene-based butane plastomer. They mitigated the problem of sample sagging in the rheometer by quenching the samples after stretching with water. The results of their experiments showed that a higher degree of crystallization could be achieved by stretching samples at a temperature near the peak melting temperature. These results were also explained by increased mobility of polymer chains at high temperatures (Sentmanat et al. 2010). One of the difficulties of studying extensional-flow-induced crystallization falls in the design of an experiment which includes a well-defined extensional flow and well-defined temperature protocol (Hadinata et al. 2007). Due to sample sagging, SER extensional rheometers are not suitable for studies that require the preservation of samples for crystallization analysis. Although the samples can be quenched with water to solidify them before sagging occurs, we feel that a more ideal temperature protocol is necessary for flow induced crystallization measurements.

Recently, Chellamuthu et al. (2011) was able to perform extensional-flow-induced crystallization measurements of isotactic poly-1-butene using the same filament stretching rheometer and oven described in this paper. Even though their samples did not display significant strain hardening or extensional thickening, they found that the application of extensional flow had significant effects on crystallization of the polymer. Using a differential scanning calorimeter, they measured that the degree of crystallinity increased from 45% to 62% with an increase in extension rate from $\dot{\varepsilon} = 0.01\ s^{-1}$ to $\dot{\varepsilon} = 0.50\ s^{-1}$ for a fixed imposed strain. They also found that there was a critical extension rate below which no flow-induced crystallization occurred. More interestingly, they found that there exists an extension rate for which the percent crystallization was maximized. Above this maximum, the percent crystallization decreased to a value which was still greater than the percent crystallization obtained for the quiescent case. One of the objectives of this study is to determine if this trend is specific to poly-1-butene or if it is robust and exists in other polymers as well.

In addition to DSC measurements, Chellamuthu et al. (2011) also performed small-angle X-ray scattering (SAXS) of the crystallized samples. The results of the SAXS experiments showed the presence of a highly oriented crystal structure in samples which had experienced high extension rates, demonstrating the development of a shish-kebab morphology as a result of molecular alignment caused by the application of strong extensional flow. They attributed the observed increase in percent crystallization to the increase in deformation caused by the flow and resulting in the strengthening of the thread-like precursors which lead to the growth of a shish-kebab crystal structure. The results of these experiments demonstrate the ability of extensional flows to align the contour path of polymer chains, stretch polymer chains, develop the thread-like precursors required for the growth of shish-kebabs, and increase nucleation points. In this paper, the criteria for the development of shish-kebabs in extensional flows will be studied for isotactic polypropylene and the impact of crystalline morphology on the presence of the maximum in the percent crystallization will be investigated.

The investigation of flow-induced crystallization of isotactic polypropylene by use of a filament-stretching rheometer is the focus of this research. In the sections of this paper that follow, the experimental processes for characterizing changes in percent crystallization through the use of filament-stretching extensional rheology methods are described. The paper concludes with a discussion about the results of the experiments.

Experimental setup

Materials

Extensional-flow-induced crystallization was studied for a commercial grade isotactic polypropylene (PP) melt (Borealis HB205TF). The material was provided by Borealis in the form of pellets and was free of nucleating agents. The PP has a molecular weight of $M_w = 600{,}000$ g/mol and a polydispersity of 4.2. The entanglement molecular weight is on the order of $M_e = 7{,}000$ g/mol. Before being tested in the shear and extensional rheometers, the pellets were first molded to fit the plate geometry in a hot press under vacuum at 200°C.

Filament-stretching extensional rheometry and experimental methods

A filament-stretching extensional rheometer (FiSER) was used to apply a homogeneous uniaxial extensional flow to the melts. Transient force and midpoint radius were measured simultaneously as the fluid filament, placed between its two end plates, was stretched. A schematic of the filament-stretching rheometer and oven is shown in Fig. 1. A complete description of the design and operating space of the filament-stretching rheometer used in these experiments can be found in the literature (Chellamuthu et al. 2011; Rothstein 2003; Rothstein and McKinley 2002a, b) and a more detailed history of the technique can be found in the following papers by the McKinley and Sridhar groups (Anna et al. 2001; McKinley and Sridhar 2002b; Tirtaatmadja and Sridhar 1993).

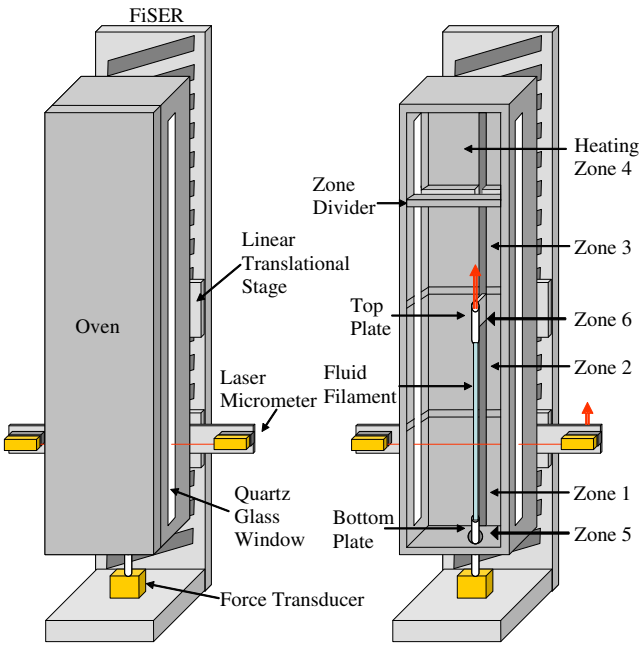

Fig. 1 Schematic diagram of a filament stretching rheometer with custom-built oven

The objective of these extensional-flow-induced crystallization measurements was to impose a constant extension rate on the fluid filament. A PID controller is used to command the endplate velocity based on measurements taken of diameter to maintain a constant extension rate. The system is able to control the diameter within 10% of the required diameter and extension rates for extension rates up to $\dot{\varepsilon} = 1.0\ \mathrm{s}^{-1}$ and down to diameters of approximately $D = 100\ \mu$m. The deformation imposed upon the fluid filament can be described in terms of a Hencky strain, $\varepsilon = -2\ln(R_{\mathrm{mid}}/R_0)$, where R_0 is the initial midpoint radius of the fluid filament. In order to calculate the extensional viscosity, the elastic tensile stress difference generated within the fluid filament was calculated from the total force measured by the load cell mounted to the bottom endplate and the diameter of the fluid filament measured along the axial.

In order to apply filament stretching techniques to polymer melts, an oven was designed and integrated with the filament-stretching rheometer (Chellamuthu et al. 2011). A schematic of the filament-stretching rheometer and oven is shown in Fig. 1. The oven is designed such that the fluid filament is fully enclosed as it is stretched. Some modifications to the described in Chellamuthu et al. (2011) were required to control the temperature to ±1°C throughout the oven. In addition to the four independently controlled vertically zones which are separated by horizontal plates to reduce natural convection, two local heating zones were added to the endplates. One zone consists of a band heater surrounding the bottom plate. The other consists of a cartridge heater built into the top plate; allowing the heater to translate with the motion of the top plate. The placement of these two zones mitigated the conductive heat losses through the top and bottom endplates.

The Janeschitz-Kriegl protocol was implemented to study flow-induced crystallization of isotactic polypropylene. Samples were initially heated from room temperature to a temperature of 200°C, 34.4°C above the peak melting temperature of 165.6°C, at a rate of 17.5 K/min and held for an additional 5 min to erase any thermal and mechanical histories. Increasing the temperature and hold time would increase the certainty that all of the crystals are fully broken down; however, these factors lead to increased sagging and likelihood of degradation of the sample. After holding at 200°C, the samples are then quenched to a

temperature that will allow crystallization of the sample. The goal is to study the effect of flow on the nucleation process, not to introduce large crystals during the flow. Therefore, the crystallization temperature must be chosen such that crystallization does not occur during the stretch and also so crystallization can occur in a time that is convenient for testing. The crystallization temperature was chosen to be $T_c = 146°C$. At this temperature, crystallization at the quiescent state takes approximately 825 min and the longest stretch time used in studying changes in percent crystallization was 40 s. Note that the imposition of flow accelerates crystallization kinetics and crystallization of the samples was observed to occur shortly after cessation of flow. The samples were quenched at a rate of 5 K/min and allowed to equilibrate; the total quenching and equilibration time was 15 min. At this time, a well-defined extensional strain was applied. The samples were held at the crystallization temperature for an additional 5 min (including stretch time). The midsections of the samples were fully crystallized after this time. However, the portions of the samples near the endplates, which did not experience the same flow history as the midsections, were not crystallized. To be conservative, a second quenching procedure was added to crystallize and solidify the remaining portions of the samples. From the crystallization temperature, the samples were quenched to 127°C at a rate of 2 K/min and held for an additional 5 min; at this time, the sample was cooled to room temperature and removed from the fixture. All DSC, microscopy, and SAXS measurements were performed on samples cut from the middle of the crystallized filament.

Results and discussions

Shear rheometry

The linear viscoelasticity of the polymer melts was measured using a commercial rotational rheometer (Stresstech, ATS Rheosystems) with a 25-mm parallel plate geometry. A master curve was compiled of frequency sweeps performed at 10° increments from 150°C to 210°C. Time–temperature superposition was then used to construct storage modulus, G', and loss modulus, G'', curves for the polymer melt at the crystallization temperature, $T_c = 146°C$. The storage modulus is a measure of the materials elastic response to shear, while the loss modulus is a measure of its viscous response. The master G' and G'' curves and complex viscosity, η^*, curve are presented in Fig. 2 and are characteristic of an entangled polymer melt.

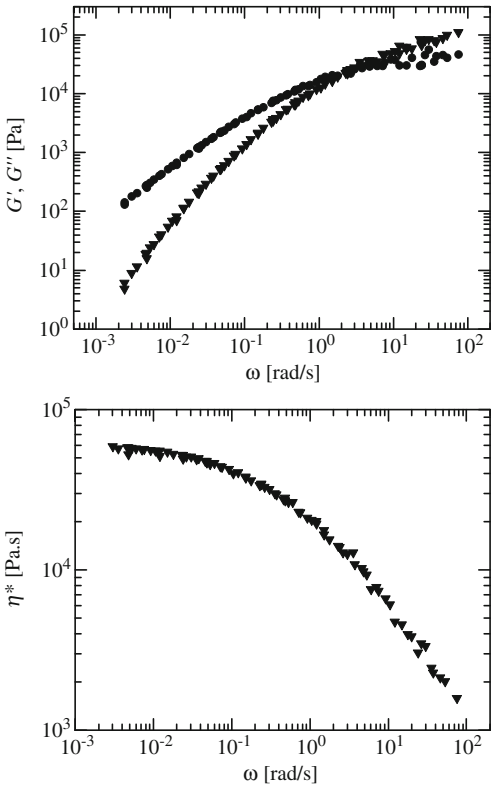

Fig. 2 The oscillatory shear master curves for isotactic polypropylene at $T_c = 146°C$. *Above* are the solutions of modulus master curves with storage modulus, G' (*black down-pointing triangle*), and loss modulus, G'' (*black circle*). *Below* is the master curve with dynamic viscosity, η^*

The viscoelastic response was used to determine the relaxation times of the polymer at the crystallization temperature, $T_c = 146°C$. The disengagement time was determined by fitting a multi-mode Maxwell model to the G' and G'' curves. A spectrum of relaxations times, λ_i, modulus coefficients, G_i, and viscosities, $\eta_i = \lambda_i G_i$, were obtained using the Iris Rheo-Hub software. A viscosity-weighted average relaxation time, $\lambda_d = \sum_{i=1}^{n} \lambda_i \eta_i / \sum_{i=1}^{n} \eta_i$, was taken in order to account for the relative importance of each mode. The disengagement time for the isotactic polypropylene sample studied was found to be $\lambda_d = 7.6$ s and the zero-shear-rate viscosity was found to be $\eta_0 = 5.8 \times 10^4$ Pa · s.

Filament-stretching rheometry

To investigate the effect of extension rate and Weissenberg number on crystallization, the polymer melts were stretched at extension rates ranging from $0.075\ s^{-1} < \dot{\varepsilon} < 0.75\ s^{-1}$ to strains of up to $\varepsilon \approx 5$. Extension rates below $\dot{\varepsilon} = 0.075\ s^{-1}$ could not be studied because crystallization of the sample was observed

to occur during the stretch. Extension rates above $\dot{\varepsilon} = 0.75\ \mathrm{s}^{-1}$ could not be studied due to excessive diameter decay post stretch as a result of the instability of the fluid filaments developing at high extension rates. This instability also limited the strains that could be reached at the higher extension rates. As a result, a final strain of $\varepsilon = 3$ was chosen for all of the extensional-flow-induced crystallization experiments to ensure that measurements over a full decade of extension rates could be performed while maintaining a coherent fluid filament for subsequent DSC and SAXS measurements. The observed high extension rate instability is known in the literature to occur as a result of Considère's criterion (McKinley and Hassager 1999) and is likely due to slipping of highly oriented polymer chains at high Weissenberg numbers. As a result of this instability, extension rates faster than the inverse of the Rouse time ($\lambda_R \sim 0.03$ s) could not be achieved and thus, although alignment of polymer chains is expected, measurements for melts experiencing polymer stretch were not possible. Hassager et al. (1998) showed that, using a fast PID control system, measurements beyond the onset of this necking instability could still be made. Unfortunately, the control system used in this study was not fast enough to be employed to explore beyond the onset of necking instability.

Extensional viscosity is plotted as function of time for a variety of extension rates in Fig. 3 with the linear viscoelastic limit superimposed over the data. Only the slowest experiments were observed to reach steady state before filament failure. Modest strain hardening and deviation from the linear viscoelastic limit were observed for all extension rates tested with the deviation occurring at earlier times with increasing extension rate. As the accumulated Hencky strain is increased, it can be seen from Fig. 3 that the maximum extensional viscosity achieved before fluid failure does not vary monotonically with extension rate. Instead, it initially increases with increasing extension rate before going through a maximum and decreasing at higher extension rates. These trends are in agreement with previous experimental observations and constitutive models for extensional rheology of entangled linear polymer melts (Bhattacharjee et al. 2002).

In Fig. 4, the extensional viscosity is plotted against extension rate, while in Fig. 5 the data is non-dimensionalized to show the Trouton ratio, $Tr = \eta_E(\varepsilon = 3)/\eta\left(\dot{\gamma} = \sqrt{3}\dot{\varepsilon}\right)$ as a function of Weissenberg number. Here the Trouton ratio is evaluated using the value of the extensional viscosity achieved at an accumulated strain of $\varepsilon = 3.0$. This value of strain was chosen instead of the maximum strain achieved before filament failure because it coincides with the total strain imposed on the samples during the extensional-flow-induced crystallization experiments. As such, they provide information about the deformation and alignment of the polymer melt during crystallization. For entangled polymer systems, at Weissenberg numbers greater than $Wi > 1/2$, the flow has become strong enough to align the contour path of the polymer chains, but not strong enough to significantly stretch the polymers. For Weissenberg numbers in the range of $1/2 < Wi < 1$, the Trouton ratio is observed to increase from the linear viscoelastic limit and plateau at a value of approximately $Tr \approx 10$. Due to the shear thinning nature of the polymer melt, this plateau in Trouton ratio corresponds to a slight thinning of the extensional viscosity as seen in Fig. 4. These results suggest that the

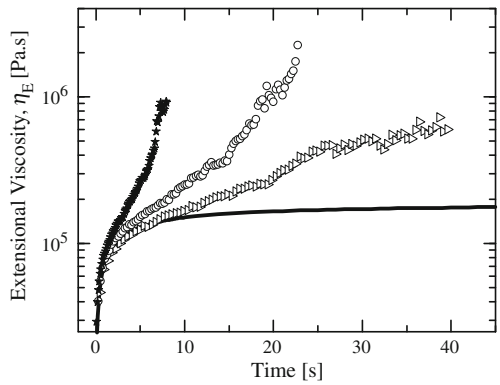

Fig. 3 Filament stretching extensional rheology measurements of extensional viscosity as a function of time for isotactic polypropylene melts stretched at various extension rates at $T_c = 146°\mathrm{C}$. Included are the results for extension rates of $\dot{\varepsilon} = 0.11\ s^{-1}$ (*white right-pointing triangle*), $\dot{\varepsilon} = 0.15\,s^{-1}$ (*white circle*), and $\dot{\varepsilon} = 0.38\,s^{-1}$ (*black star*). The *solid line* represents the linear viscoelastic response

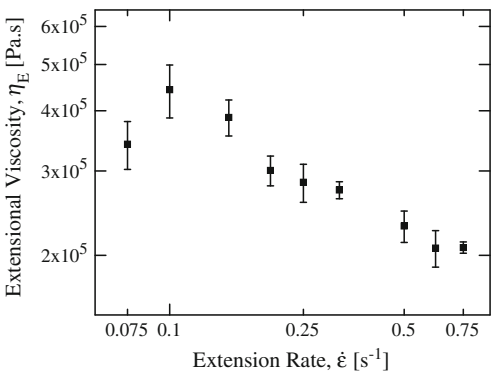

Fig. 4 Filament stretching extensional rheology measurements of extensional viscosity as a function of extension rate for polypropylene melts stretched at $T_c = 146°\mathrm{C}$ to a fixed strain of $\varepsilon = 3.0$

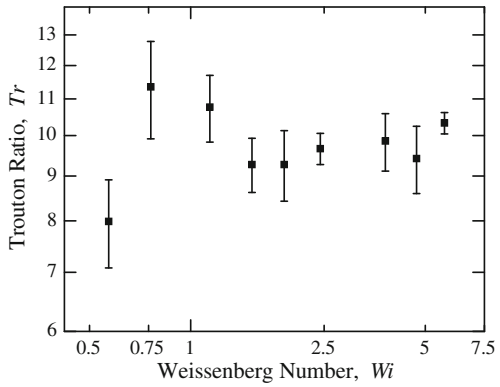

Fig. 5 Filament stretching extensional rheology measurements of Trouton ratio as a function of Weissenberg number for isotactic polypropylene melts stretched at $T_c = 146°C$ to a fixed strain of $\varepsilon = 3.0$

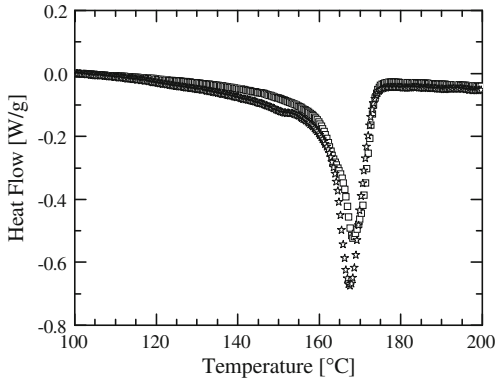

Fig. 6 DSC measurements showing heat flow as a function of temperature. Included are isotactic polypropylene samples crystallized under quiescent conditions (*open square*) and following a stretch with an extension rate of $\dot{\varepsilon} = 0.25\,s^{-1}$ at a fixed strain of $\varepsilon = 3.0$ (*star*)

extensional flow is not fast enough to cause much deformation of the polymer chains because of the absence of significant extensional thickening at high Weissenberg numbers (Rothstein and McKinley 2002a).

Crystallization measurements

Differential scanning calorimetry (DSC) was performed on the crystallized samples to determine percent crystallization using a TA Instruments model DSC 1. All experiments were performed under purged nitrogen and samples were heated from 25°C to 200°C. The samples were first heated at a rate of 10 K/min up to 100°C. A slower rate of 1 K/min was used from 100°C to 200°C, as this is the temperature range of most interest. DSC measurements were performed on the isotactic polypropylene samples post-stretch and crystallization to determine the degree of crystallinity. The results were compared to the DSC measurements of quiescent samples, which experienced the same thermal history as the stretched samples in the absence of extensional flow. In Fig. 6, two DSC measurements are presented, one for a quiescent case, the other for an extension rate of $\dot{\varepsilon} = 0.25\ s^{-1}$. The area enclosed by the melt curve gives the latent heat of fusion, ΔH, of the sample, which is used to calculate percent crystallization. In this case, the energy required to melt the stretched sample was found to be significantly larger than the energy required to melt the quiescent sample. The percent crystallization is calculated from the DSC data as $\Delta H/\Delta H_u$, where $\Delta H_u = 209$ J/g (Quirk and Alsamarraie 1989) is the heat of fusion per unit mass for complete crystallization of isotactic polypropylene.

Percent crystallization is reported in Fig. 7 as a function of Weissenberg number for samples stretched to a final strain of $\varepsilon = 3.0$ as well as for quiescent samples. Percent crystallization begins to increase from the quiescent state at the critical Weissenberg number of approximately $Wi = 1$ and continues to increase to a maximum at the peak Weissenberg number of approximately $Wi = 2$. This maximum of 52% crystallinity represents an increase of approximately 18% above the quiescent case. A similar maximum was observed by Chellamuthu et al. (2011) for two different poly-1-butene samples. Thus, it appears that this phenomenon is not characteristic of only poly-1-butene and may prove to be a robust phenomenon independent of the polymer and its degree of polydispersity. After the maximum, the percent crystallization decreases to a plateau which is only slightly more crystalline than the quiescent case. This initial onset of increase in percent crystallization at $Wi = 1$ was also observed by Chellamuthu et al. (2011). DSC was also used to examine the changes in peak melting temperature as

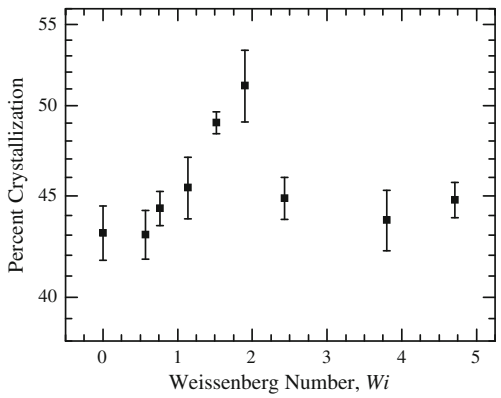

Fig. 7 Percent crystallization as a function of extension rate and Weissenberg number for isotactic polypropylene samples crystallized following stretches to a fixed strain of $\varepsilon = 3.0$

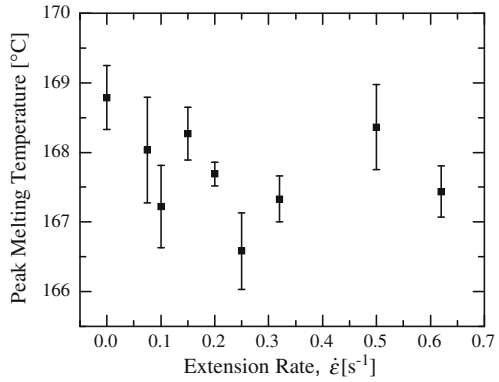

Fig. 8 Peak melting temperature as a function of extension rate for isotactic polypropylene samples crystallized following stretches of various extension rates to a fixed strain of $\varepsilon = 3.0$

a result of increasing extension rate. The results are shown in Fig. 8. A general decrease in peak melting temperature from the quiescent case was observed until the peak extension rate. After this extension rate, the peak melting temperature displays a general increase although the variation in the data is enough to obscure the trends. This is quite different from the work of Chellamuthu et al. (2011) who found a sharp increase in the peak melting temperature with increasing extension rate corresponding to a transition from spherulite to shish-kebab crystals.

Optical microscopy (Nikon TE200-U) was performed through crossed polarizers to qualitatively characterize changes in spherulite size, numbers, and crystalline structure as a result of the application of extensional flow. Spherulitic crystals appear in the polarized microscopy images as Maltese crosses, as shown in Fig. 9. The microscopy images show an increase in the number of spherulites and the decrease in spherulite size with increasing extension rate up to the peak extension rate, $\dot{\varepsilon} = 0.25\ \mathrm{s}^{-1}$. This observation suggests an increased nucleation density with increased extension rate. No change in spherulite size or number was observed from the quiescent case for extension rates below the critical extension rate. After the peak extension rate, changes to spherulite size and numbers appeared to cease. No signs of a highly oriented shish-kebab structure in the flow direction could be inferred from the microscopy images. Thus, scattering measurements were required to determine the final crystalline structure.

Small-angle X-ray scattering was also performed on the samples to investigate the effect of extensional flow on the structure and alignment of the polymer crystals. SAXS measurements were performed using an instrument from Molecular Metrology Inc. (Rigaku S-Max3000). The X-ray beam was 0.40 mm in diameter with a wavelength of $\lambda = 0.1542$ nm. The sample to detector distance was calibrated using silver behenate standard peak at wave vector of $q = 1.076\ \mathrm{nm}^{-1}$, where $q = \left(4\pi/\lambda\right)\sin\theta$ and 2θ is the scattering angle. The samples were placed in the instrument such that measurement was taken at the axial center of the filament and the flow direction was aligned perpendicular to the beam direction; this allows any crystal alignment in the flow direction to be detected in the two-dimensional scattering patterns. SAXS was performed for a number of samples for each extension rate examined. Several characteristic scattering patterns and scattering intensity versus wave vector, q, are shown for an extension rate below and an extension rate above the critical extension rate in Figs. 10 and 11, respectively. All of the scattering patterns showed equally spaced

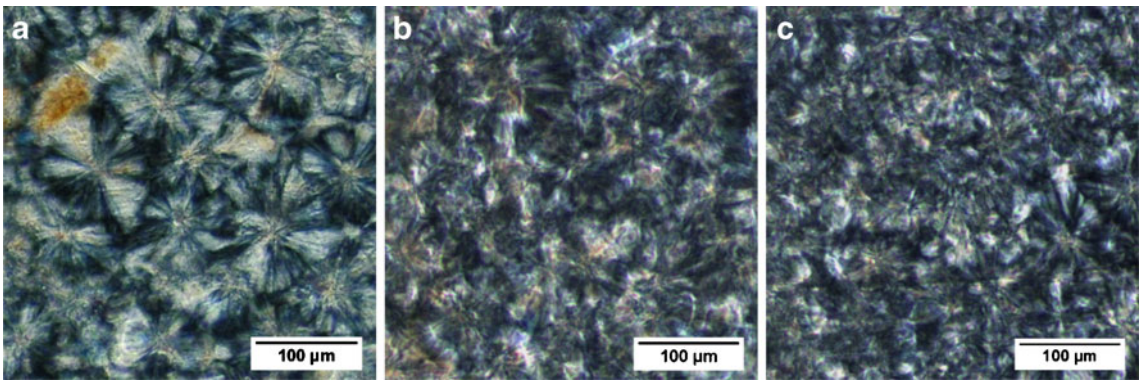

Fig. 9 Microscopy images taken through crossed polarizers of isotactic polypropylene samples showing the size of spherulites under **a** quiescent conditions and following stretches with extension rates of **b** $\dot{\varepsilon} = 0.10\,\mathrm{s}^{-1}$, and **c** $\dot{\varepsilon} = 0.25\,\mathrm{s}^{-1}$ at a fixed strain of $\varepsilon = 3.0$. The direction of flow is aligned vertically

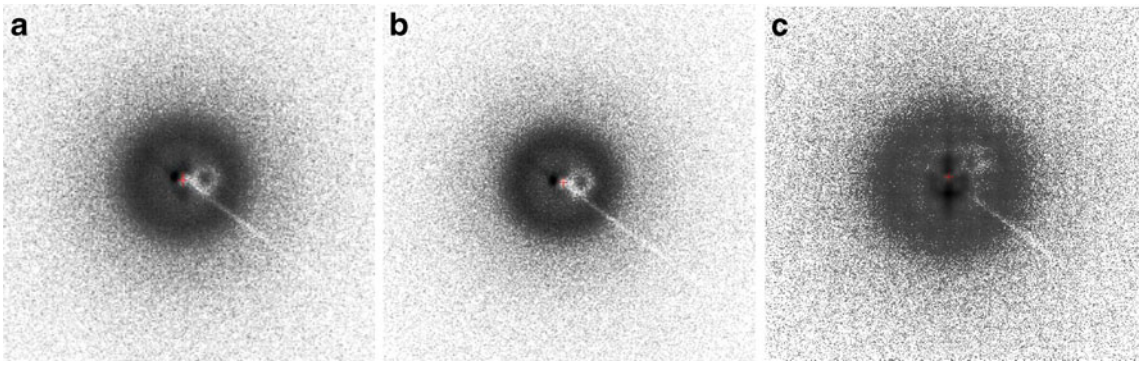

Fig. 10 Two dimensional small-angle X-ray scattering patterns for isotactic polypropylene samples crystallized following stretches with extension rates of **a** $\dot{\varepsilon} = 0.075\,\mathrm{s}^{-1}$ and **b** $\dot{\varepsilon} = 0.25\,\mathrm{s}^{-1}$ to a final strain of $\varepsilon = 3.0$ and an extension rate of **c** $\dot{\varepsilon} = 0.25\,\mathrm{s}^{-1}$ to a final strain of $\varepsilon = 4.0$. The stretch direction is aligned horizontally to the scattering patterns

axisymmetric rings, which are indicative of a lamellar crystal structure (Lyngaae-Jsrgensen and Sondergaard 1995). The d-spacing of the lamellar stacks was measured to decrease slightly from 23 to 22 nm between extension rates of $\dot{\varepsilon} = 0.075\ \mathrm{s}^{-1}$ and $\dot{\varepsilon} = 0.25\ \mathrm{s}^{-1}$, respectively. The maximum effect on d-spacing was found to occur at the transition to the critical extension rate where a large increase in crystallinity was observed. Little or no effect was observed between extension rates above the critical extension rate. This observation is not completely unexpected because it has been shown in shear flow that for monodisperse polymers, the formation of shish-kebab morphologies are only possible for flows where $\dot{\gamma} > 1/\lambda_R$ (Mykhaylyk et al. 2011; van Meerveld et al. 2004) and all of the experiments here are for $1/\lambda_d < \dot{\gamma} < 1/\lambda_R$. However, for highly polydisperse systems like the poly-1-butylene melts studied by Chellamuthu et al. (2011), shish-kebab morphologies can be generated if the specific work imposed by the shear or extensional flow is large enough to adequately deform the higher molecular weight fractions of the melt thereby generating the highly aligned shish nuclei on which the lower molecular weight fraction of the polymer can crystallize as kebabs (Mykhaylyk et al. 2010). What is interesting about this observation is that a maximum in percent crystallinity of the isotactic polypropylene sample was observed even without the formation of a shish-kebab morphology in the final solid.

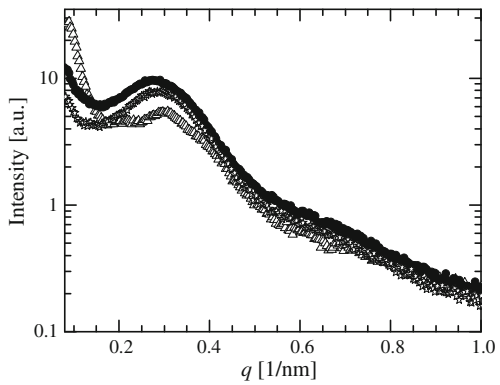

Fig. 11 Intensity of the scattering images presented in Fig. 10 as a function of scattering vector, q, for isotactic polypropylene samples crystallized following stretches with extension rates of $\dot{\varepsilon} = 0.075\,\mathrm{s}^{-1}$ (*close circle*) and $\dot{\varepsilon} = 0.25\,\mathrm{s}^{-1}$ (*open triangle*) to a final strain of $\varepsilon = 3.0$ and an extension rat of $\dot{\varepsilon} = 0.25\,\mathrm{s}^{-1}$ (*star*) to a final strain of $\varepsilon = 4.0$

By applying the Janeschitz-Kriegl protocol for a range of strains at select extension rates, the effect of varying strain and increased specific work was characterized. An extension rate of $\dot{\varepsilon} = 0.25\ \mathrm{s}^{-1}$, for which the maximum percent crystallization was observed at a strain of $\varepsilon = 3.0$, was chosen to examine the changes in percent crystallization as a result of varying strain in the range of $\varepsilon = 2.0$ to $\varepsilon = 4.0$ and to determine if an increase in strain would lead to the formation of a shish-kebab crystal structure. In addition, strains were applied in the range of $\varepsilon = 3.0$ to $\varepsilon = 4.0$ for an extension rate of $\dot{\varepsilon} = 0.075\ \mathrm{s}^{-1}$, for which no change in crystallization was observed from the quiescent state at a strain of $\varepsilon = 3.0$, to investigate if an increase in strain would lead to an increase in crystallization. The magnitude of accumulated strain was limited to $\varepsilon = 4.0$ for both extension rates, due to instabilities that ensued at high strains and the limits of the PID control system. For both extension rates, a modest increase in crystallization of a couple percent was observed with increasing extensional strain; however, in neither case was the trend significant when compared to the uncertainty in

the data. Additionally, SAXS measurements showed that even at a strain of $\varepsilon = 4.0$, neither extension rate resulted in the creation of shish-kebabs. Furthermore, no significant effect on d-spacing was observed as a result of increase in strain.

In order to better understand the crystallization dynamics under extensional flow, the time required for crystallization to occur during flow was directly measured for isotactic polypropylene. This was accomplished by stretching the isotactic polypropylene melts for times great enough for crystallization of the samples to occur during the extensional flow. These experiments violate the Janeschitz-Kriegl protocol, but provide insight into the rate of crystal nucleation and growth under extensional-flow-enhanced crystallization. In the experiment, the time of crystallization was marked by the time at which a sudden increase in the measured force was observed. This approach was similar to that used by Hadinata et al. (2007) for poly-1-butene, where they defined the crystallization time to be the time at which a sharp increase in extensional viscosity was observed during stretching of the polymer melts. Isotactic polypropylene samples were stretched at extension rates ranging from $\dot{\varepsilon} = 0.01\ \mathrm{s}^{-1}$ to $\dot{\varepsilon} = 0.15\ \mathrm{s}^{-1}$ for accumulated Hencky strains that in some cases grew in excess of $\varepsilon = 7$. For a number of reasons, these experiments could not be performed easily using the PID controller. As a result, an exponential velocity (or type II) profile was imposed on the end-plates instead. In this type II experiment, the length of the fluid filament is commanded to follow the exponential profile $L(t) = L_0 e^{\dot{\varepsilon} t}$, where L_0 is the initial length of the fluid filament. The resulting extension rate imposed on the fluid filament can then be calculated from the radius decay.

In Fig. 12, the measured force is presented as a function of time. A sudden increase in force can be seen towards the end of the stretch; this jump in force and consequential jump in extensional viscosity was taken to be the crystallization time of the sample. The crystallization time is shown for various extension rates in Fig. 13. The range of extension rates which could be investigated was limited by sagging of the melts under gravity at extension rates below $\dot{\varepsilon} = 0.01\ \mathrm{s}^{-1}$ and by failure of the fluid filaments before crystallization could occur caused by the necking instability at high strains for extension rates above $\dot{\varepsilon} = 0.15\ \mathrm{s}^{-1}$. This corresponds to a range in Weissenberg numbers between $0.08 < Wi < 1.2$. The crystallization time was observed to decrease linearly with the inverse of the extension rate, $t_c \propto \dot{\varepsilon}^{-1}$. A similar trend and dependency on extension rate was observed by Hadinata et al. (2007). Interestingly, the decrease in the crystallization time

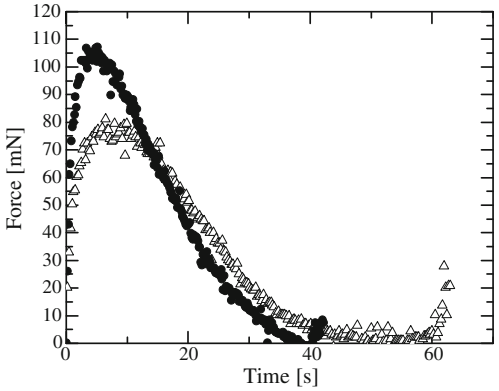

Fig. 12 FiSER measurements of force as a function of time for isotactic polypropylene samples crystallizing during extensional flows with extension rates of $\dot{\varepsilon} = 0.10\,\mathrm{s}^{-1}$(*white triangle*) and $\dot{\varepsilon} = 0.15\,\mathrm{s}^{-1}$(*black circle*) at $T_c = 146°\mathrm{C}$. The onset of crystallization is observed as an abrupt upturn in the force measurement at roughly $t = 40$ s and $t = 60$ s for extension rates of $\dot{\varepsilon} = 0.10\,\mathrm{s}^{-1}$ and $\dot{\varepsilon} = 0.15\,\mathrm{s}^{-1}$, respectively

was observed for extension rates well below the critical Weissenberg number of $Wi = 1$, where no increase in percent crystallization from the quiescent state was observed. In the work of Hadinata et al. (2007), a lower extension rate limit was found, below which flow did not affect the crystallization dynamics. However, as has been observed here, by our calculations of their average relaxation time, Hadinata et al. (2007) also found that the extensional flow influenced crystallization kinetics for Weissenberg numbers well below $Wi < 1$. At these low Weissenberg numbers, the flow should not be strong enough to cause alignment or deformation of the polymer chains. However, due to the relatively large polydispersity of these samples, it is possible that the presence of the high molecular weight polymer chains, which can have much longer relaxation times than the average, are deforming at these lower

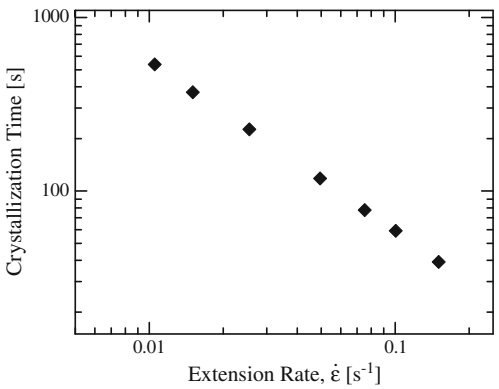

Fig. 13 Crystallization time as a function of extension rate for isotactic polypropylene

extension rates. High molecular weight tails are known to increasing the number of nucleation sights and the nucleation rate in shear flows (Seki et al. 2002). Another possibility is that the decrease in crystallization time is not due to the enhanced deformation or alignment of polymer chains, but simply the enhanced frequency of interaction between undeformed polymer chains as they are advected along by the imposed extensional flow. This might explain why at these low Weissenberg number the crystallization kinetics are affected without affecting the percent crystallinity of the sample.

If one plots the results in Fig. 13 in terms of a strain rather than a crystallization time, one finds that the onset of crystallization occurs in each experiment at the same value of extensional strain, $\varepsilon_c = t_c\ \dot{\varepsilon} = 5.8$. These measurements clearly show the upper limit of strain that can be imposed while maintaining the Janeschitz-Kriegl protocol. Interestingly, in shear flows, the strain required to initiate flow-induced crystallization is not constant, but has been shown to increase with increasing shear rate (Hadinata et al. 2007). At this point, it is not clear what the origin is for this difference between shear and extensional-flow-induced crystallization.

Conclusions

The degree of crystallization of isotactic polypropylene was found to be strongly affected by the application of extensional flow. A critical extension rate was found to be required for an increase in crystallization to occur. At this critical extension rate, the Weissenberg number had reached $Wi = 1$ and the flow was strong enough to align the contour path of the polymer chains. The critical extension rate corresponds to the maximum Trouton ratio, which verifies the occurrence of alignment along the contour polymer chains in the flow direction. Percent crystallization increased to a maximum, which was 18% greater than the quiescent case, at the peak extension rate. After the maximum, the percent crystallization decreased to a plateau. In this region the percent crystallization was a few percent greater than the quiescent case. Polarized light microscopy verified an increase in the number of spherulites and decrease in spherulite size for extension rates at or above the critical extension rate. Microscopy also showed a continued increase in number and decrease in size of spherulites until the peak extension rate at which the maximum percent crystallization occurs. No apparent change in spherulite size or number was observed for extension rates above the peak extension rate.

Small-angle X-ray scattering was used to investigate the crystal structure of the stretched isotactic polypropylene samples. The scattering patterns of all of the samples examined displayed a lamellar crystal structure which is indicated by an azimuthally symmetric scattering pattern with radially spaced bright rings. A 7% decrease in d-spacing was observed at the transition to the critical extension rate. Inter-lamellar spacing was not found to be greatly influenced by the strength of flow as it was not observed to change for an increase in extension rate past the critical extension rate.

The trends in percent crystallization for varying extension rates are similar to those found by Chellamuthu et al. for poly-1-butene (Chellamuthu et al. 2011), even though a shish-kebab structure was not detected for any of the samples in the SAXS measurements or polarized light microscopy images. This suggests that the maximum in percent crystallization is not dependent on the formation of a shish-kebab crystal structure, as suggested by Chellamuthu et al. (2011), but is a more general result for a wide spectrum of polymers. It is interesting to note, however, that the plateau in percent crystallization for poly-1-butene, which possessed a shish-kebab crystal structure, was still 10–20% greater than the quiescent case (Chellamuthu et al. 2011). The plateau in percent crystallization for isotactic polypropylene was only a few percent greater than the quiescent case. These results suggest that in some cases the formation of a shish-kebab crystal structure can lead to a greater degree of crystallinity in the final state.

The dynamics of crystallization for isotactic polypropylene were also studied. The time required for the onset of crystallization was found to be linearly proportional to the inverse of extension rate. As a result, the onset of crystallization was found to occur at a constant value of strain, $\varepsilon_c = 5.8$ across all extension rates tested. This was true even for extension rates well below a Weissenberg number of $Wi < 1$ where little polymer deformation is expected and where no increase in percent crystallization from the quiescent state was observed. This is likely to be either the result of polydispersity of the polymer where high molecular weight polymers can have much longer relaxation times and thus locally experience a flow with Weissenberg numbers well above $Wi > 1$ or it is the result of an increased interaction between undeformed polymers as they are advected by the imposed extensional flow.

Acknowledgements The authors would like to thank the National Science Foundation for the generous support of this research under grant CBET-0651888, CTS-0547180, and the

UMASS MRSEC for the use of their DSC and shear rheology facilities. Finally, the authors would like to thank Vikram K. Daga for his help with SAXS measurements.

References

Anna SL, McKinley GH, Nguyen DA, Sridhar T, Muller SJ, Huang J, James DF (2001) An inter-laboratory comparison of measurements from filament stretching rheometers using common test fluids. J Rheol 45:83–114

Bhattacharjee PK, Oberhauser J, McKinley GH, Leal LG, Sridhar T (2002) Extensional rheometry of entangled solutions. Macromol 35:10131–10148

Chellamuthu M, Arora D, Winter HH, Rothstein JP (2011) Extensional flow induced crystallization of isotactic poly-1-butene using a filament stretching rheometer. J Rheol 55(4):901

Doi M, Edwards SF (1986) The theory of polymer dynamics. Oxford University Press, Oxford

Haas TW, Maxwell B (1969) Effects of shear stress on crystallization of linear polyethylene and polybutene-1. Polym Eng Sci 9:225

Hadinata C, Boos D, Gabriel C, Wassner E, Rullmann M, Kao N, Laun M (2007) Elongation-induced crystallization of a high molecular weight isotactic polybutene-1 melt compared to shear-induced crystallization. J Rheol 51:195–215

Hassager O, Kolte MI, Renardy M (1998) Failure and nonfailure of fluid filaments in extension. J Non-Newton Fluid Mech 76:137–151

Janeschitz-Kriegl H (2003) How to understand nucleation in crystallizing polymer melts under real processing conditions. Colloid Polym Sci 281:1157–1171

Janeschitz-Kriegl H, Covas JA, Agassant JF, Diogo AC, Vlachopoulos J, Walters K (1995) Polymer crystallization under process conditions. Rheological fundamantals of polymer processing. Kluwer Academic Publishers, Dordrecht

Keller A, Kolnaar HWH (1997) Flow-induced orientation and structure formation. Wiley-VCH, New York

Lyngaae-Jsrgensen J, Sondergaard K (1995) Theories of small-angle light, X-ray, and neutron scattering. Rheo-physics of multiphase polymeric systems. TECHNOMIC Publishing Co., Lancaster

Mackley MR (1975) Shish-Kebabs—hydrodynamic factors affecting their crystal-growth. Colloid Polym Sci 253:373–379

Mackley MR, Keller A (1975) Flow induced polymer-chain extension and its relation to fibrous crystallization. Philos Trans R Soc Lond Ser A: Math Phys Eng Sci 278:29

McKinley GH, Hassager O (1999) The Considere condition and rapid stretching of linear and branched polymer melts. J Rheol 43:1195–1212

McKinley GH, Sridhar T (2002a) Filament-stretching rheometry of complex fluids. Annu Rev Fluid Mech 34:375–415

McKinley GH, Sridhar T (2002b) Filament stretching rheometry. Annu Rev Fluid Mech 34:375–415

Mykhaylyk OO, Chambon P, Impradice C, Fairclough JPA, Terrill NJ, Ryan AJ (2010) Control of structural morphology in shear-induced crystallization of polymers. Macromolecular 43:2389–2405

Mykhaylyk OO, Fernyhough CM, Okura M, Fairclough JPA, Ryan AJ, Graham R (2011) Monodisperse macromolecules—a stepping stone to understanding industrial polymers. Eur Polym J 47:447–464

Quirk RP, Alsamarraie MAA (1989) Physical constants of poly(propylene). In: Brandup J, Immergut EH (eds) Polymer handbook. Wiley, New York

Rothstein JP (2003) Transient extensional rheology of wormlike micelle solutions. J Rheol 47:1227–1247

Rothstein JP, McKinley GH (2002a) A comparison of the stress and birefringence growth of dilute, semi-dilute and concentrated polymer solutions in uniaxial extensional flows. J Non-Newton Fluid Mech 108:275–290

Rothstein JP, McKinley GH (2002b) Inhomogeneous transient uniaxial extensional rheometry. J Rheol 46:1419–1443

Seki M, Thurman DW, Oberhauser JP, Kornfield JA (2002) Shear-Mediated crystallization of isotactic polypropylene: the role of long chain-long chain overlap. Macromolecular 35:2583–2594

Sentmanat M, Delgadillo-Velazquez O, Hatzikiriakos SG (2010) Crystallization of an ehtylene-based butene plastomer: the effect of unixatial extension. Rheol Acta 49:931–939

Tirtaatmadja V, Sridhar T (1993) A filament stretching device for measurement of extensional viscosity. J Rheol 37:1133–1160

van Meerveld J, Peters GWM, Hütter M (2004) Towards a rheological classification of flow induced crystallization experiments of polymer melts. Rheol Acta 44:119–134

Van Puyvelde P, Langouche F, Baert J (2008) Flow-induced crystallization in poly-1-butene: the shish-kebab transition. Int J Mater Form 1:667–670